https://doi.org/10.3311/PPch.38170

Periodica Polytechnica Chemical Engineering, 68(4), pp. 655–664, 2024

Modeling of a PEM Electrolyzer Operating at Part Load Conditions for Dynamic Simulation in DWSIM

Igor Bzovsky[1*], Serhii Kudriavtsev[1]

[1] Department of Chemical Engineering and Ecology, Faculty of Engineering, Volodymyr Dahl East Ukrainian National University, 17 Ioanna Pavla II Street, 01042 Kyiv, Ukraine
[*] Corresponding author, e-mail: asp-161-23-14@snu.edu.ua

Received: 23 August 2024, Accepted: 18 October 2024, Published online: 11 November 2024

Abstract

The development and integration of renewable energy sources have created a growing need for efficient and flexible energy storage solutions. Proton exchange membrane (PEM) electrolysis offers a promising method for hydrogen production, a key component in the future of sustainable energy. This study focuses on the modeling and dynamic simulation of a PEM electrolyzer operating under part-load conditions using DWSIM, an open-source process simulation software. The ability of a PEM electrolyzer to operate at 10–100% of its nominal power allows for adjusting energy consumption based on current electricity prices. The primary objective is to develop a comprehensive model that represents the behavior of a PEM electrolyzer under varying operational conditions, particularly when the system is not functioning at full capacity. Considering that increasing the supplied power reduces the PEM electrolyzer efficiency due to the increase in overpotentials, the model should be optimized for the most cost-effective energy consumption. The results show that increasing the PEM stack operating temperature reduces both energy consumption and hydrogen production costs. Reducing hydrogen demand lowers energy consumption and production costs, due to the greater part-load flexibility, optimizing PEM electrolyzer operation during low electricity price periods.

Keywords

PEM electrolyzer, DWSIM, electrolysis, dynamic simulation, optimization

1 Introduction

The increasing global demand for sustainable energy solutions has positioned hydrogen as a pivotal element in the transition towards a low-carbon economy. Today 96% of hydrogen is produced from fossil fuels [1, 2]. The world demand for hydrogen amounts to 94 million tonnes, 62% of which is produced by steam reforming of natural gas, 18% is obtained as a byproduct of naphtha reforming, 19% by gasification of coal and only 35 kt hydrogen are produced by water electrolysis [3]. Hydrogen Insight forecasts that global hydrogen demand will more than triple by 2050. This significant increase will primarily be driven by sectors such as aviation, power generation and energy storage, heavy industry and transport [4].

Water splitting using electrolysis is the main technology for producing green hydrogen, alternatively, water can also be split using other energy sources, such as thermal energy (thermolysis), light energy (photoelectrolysis), and biophotolysis [5]. Currently proton exchange membrane (PEM) and alkaline electrolyzers are the most widely used water electrolysis technologies, anion exchange membrane (AEM) and solid oxide electrolyzers (SOE) are emerging technologies still in the early stages of development and commercialization.

Proton exchange membrane (PEM) electrolyzers have garnered significant attention in recent years due to their potential for efficient hydrogen production, especially when powered by renewable energy sources. A common way to categorize PEM electrolyzer models is based on their level of detail. Olivier et al. [6] classify electrolyzer models into submodels, each focusing on different aspects, such as the electrical, thermal, fluid, and chemical processes. Among these categories, static and dynamic models can be distinguished. In the majority of cases, a static approach is preferred since the electrochemical reaction occurs within 50 ms, making dynamic effects insignificant in most situations [7]. Colbertaldo et al. [8] developed a zero-dimensional dynamic model of PEM electrolyzer using Aspen Custom Modeler for studying unsteady

Cite this article as: Bzovsky, I., Kudriavtsev, S. "Modeling of a PEM Electrolyzer Operating at Part Load Conditions for Dynamic Simulation in DWSIM", Periodica Polytechnica Chemical Engineering, 68(4), pp. 655–664, 2024. https://doi.org/10.3311/PPch.38170

behavior and the role of thermal capacity. Pfennig et. al [7] introduced a model approach which addresses an inconsistency found in the literature regarding the use of the exchange current density. In study [9] a numerical dynamic model of a complete electrolysis unit was implemented with the software Simulink [10], combining customized dynamic models of the main balance of plant components. The results showed that despite the lower specific consumption of the stack at partial load, the system showed an increase in the average net specific consumptions when the load decreases toward its minimum.

In recent years, several strategies have been developed to optimize the operating costs of electrolyzers, with a focus on improving energy efficiency and reducing operational expenses. One of the key methods is dynamic power management, where electrolyzers adjust their operation based on fluctuating electricity prices, taking advantage of periods with lower tariffs [11]. Another widely adopted approach is the integration of hybrid energy systems, combining renewable energy sources such as wind and solar power with electrolysis to reduce reliance on grid electricity and mitigate high electricity costs during peak periods. In study [12], an optimal operational strategy was developed to ensure the electrolyzer operates in its most efficient range, maximizing hydrogen production efficiency while minimizing operational costs. In study [13], a bi-level optimization framework was introduced for hydrogen production using wind and solar energy, focusing on determining the optimal capacity and operational strategy by incorporating the electrolyzer life-efficiency model. In [14] the authors proposed a layered power scheduling optimization to reasonably distribute the power of the electrolyzer and energy storage system in a hydrogen production system, where the power allocation between the PEMEL and battery energy storage system (BESS) was optimized using a non-dominated sorting genetic algorithm (NSGA-II) combined with the firefly algorithm (FA).

This paper aims to present a comprehensive approach to modeling a PEM electrolyzer operating at part load conditions using DWSIM [15]. The developed model of the electrolyzer by itself is steady-state, however it can be used in dynamic DWSIM simulation with dynamic BoP components. In this study, we apply sequential least squares quadratic programming (SLSQP) to optimize the electrolyzer load distribution in response to fluctuating electricity prices. While SLSQP is a well-established optimization technique, the novelty of this work lies in its application to the specific conditions of the Ukrainian energy market and the unique constraints of electrolyzer operation. By integrating this approach, we aim to provide a cost-effective and practical solution for hydrogen production in regions with variable electricity pricing.

2 Electrolyzer modeling

In PEM electrolysis, an electric current drives the decomposition of water, supplied to the anode, into hydrogen and oxygen [8, 16]. The half reaction which takes place on the anode side is oxygen evolution reaction:

$$2\mathrm{H_2O} \rightarrow \mathrm{O_2}\left(g\right) + 4\mathrm{H^+}\left(aq\right) + 4e^-. \tag{1}$$

The half reaction which takes place on the cathode side is hydrogen evolution reaction:

$$4\mathrm{H^+}\left(aq\right) + 4e^- \rightarrow 2\mathrm{H_2}\left(g\right). \tag{2}$$

The electrolyte used in PEM electrolyzers is a polymeric membrane, through which charge carrier (H^+) moves from anode to cathode, where hydrogen is produced [8].

For the reaction to take place work should be provided to the system. Gibbs free energy change represents the minimum reversible work required to split water and can be calculated using the following equation:

$$\Delta_r G_m = \Delta_r H_m - T \cdot \Delta_r S_m \left[\mathrm{kJ / mol}\right], \tag{3}$$

where H stands for the enthalpy, T is the temperature and S is the entropy. For electrolysis process to occur additional energy is required in the form of heat, which is described by $\mathrm{T} \cdot \Delta_r S_m$ [7]. Enthalpy change represents the total required energy.

2.1 Reversible voltage

The reversible voltage is the minimum voltage required to drive the electrolysis of water under standard conditions without any losses due to overpotentials. The minimum required energy for water splitting can be calculated from Gibbs free energy [17]. A relationship between Gibbs free energy change and reversible voltage can be established using the following equation [7, 18]:

$$U_{rev} = -\frac{\Delta_r G_m^0}{n \cdot \mathrm{F}}, \tag{4}$$

where F is the Faraday constant F = 96485.3 C/mol and n is the number of free electrons in the reaction $n = 2$. Under standard conditions U_{rev} = 1.23 V, ΔG = 237.2 kJ/mol. The negative value indicates that energy needs to be added to the system. The reaction of water decomposition will not occur if a cell voltage is less than reversible voltage.

2.2 Thermoneutral voltage

The thermoneutral voltage is the voltage at which the electrolysis process operates without heat exchange with its surroundings, all the electrical energy supplied to the system is converted into the chemical energy of the hydrogen and oxygen gases produced, and there is no need to supply or remove heat to maintain a constant temperature. A relationship between an enthalpy and thermoneutral voltage can be established using the following equation [7, 18]:

$$U_{tn} = -\frac{\Delta_r H_m^0}{n \cdot \mathrm{F}}, \tag{5}$$

where $\Delta H = 285.8$ kJ/mol and $n = 2$. Therefore $U_{tn} = 1.48$ V.

If the cell voltage is between reversible voltage U_{rev} and thermoneutral voltage U_{tn}, the additional heat is needed for the electrolysis process to take place [7]. While the thermoneutral voltage is 1.48 V, practical PEM electrolyzers usually operate at higher voltages (typically 1.8 to 2.2 V) due to activation, ohmic, and concentration overpotentials that need to be overcome to drive the reaction at a significant rate.

2.3 Cell voltage

The cell voltage is the sum of the open circuit voltage, the activation overvoltage, the ohmic overvoltage and the concentration overvoltage [8, 19]:

$$U_{\mathrm{cell}} = U_{ocv} + U_{\mathrm{act}} + U_{\mathrm{ohm}} + U_{conc}. \tag{6}$$

The cell voltage directly impacts the efficiency of the electrolyzer. Lower cell voltage generally indicates higher efficiency as less electrical energy is converted into heat.

2.4 Open circuit voltage

The open circuit voltage is the minimum cell voltage required for the electrolysis process to occur and is defined by the Nernst equation [9, 18]:

$$U_{ocv}\left(T_{\mathrm{cell}}, P_{\mathrm{cell}}\right) = \frac{\Delta G_{rev}\left(T_{\mathrm{cell}}, P_{ref}\right)}{n \cdot \mathrm{F}} + \frac{\mathrm{R} \cdot T_{\mathrm{cell}}}{n \cdot \mathrm{F}} \ln\left(q\right), \tag{7}$$

where $\Delta G_{rev}(T_{\mathrm{cell}}, P_{ref})$ is the free Gibbs energy change at cell temperature and reference pressure, R is the universal gas constant, F is the Faraday constant, n is the number of moles of electrons involved in the reaction and q is the reaction quotient. The reaction quotient can be established using the Eq. (8) [7]:

$$q = \frac{p_{\mathrm{H_2}} \cdot \sqrt{p_{\mathrm{O_2}}}}{a_{\mathrm{H_2O}}}. \tag{8}$$

In the Eq. (8) cathode and anode total pressures are used [7]:

- $p_{\mathrm{H_2}}$ – cathode total pressure,
- $p_{\mathrm{O_2}}$ – anode total pressure,
- $a_{\mathrm{H_2O}}$ – activity of water in liquid state (assumed to be 1).

2.5 Activation overvoltage

Activation overvoltage is the additional voltage required to overcome the activation energy barrier of the electrochemical reactions occurring at the electrodes of a PEM electrolyzer. The activation overvoltage can be calculated using the Butler-Volmer equation [19, 20]:

$$U_{\mathrm{act},an} = \frac{\mathrm{R}T}{a_{an} \cdot n \cdot \mathrm{F}} \cdot \ln\left(\frac{i}{i_{0,an}}\right), \tag{9}$$

$$U_{\mathrm{act},cat} = -\frac{\mathrm{R}T}{a_{cat} \cdot n \cdot \mathrm{F}} \cdot \ln\left(\frac{i}{i_{0,cat}}\right), \tag{10}$$

$$U_{\mathrm{act}} = U_{\mathrm{act},an} - U_{\mathrm{act},cat}, \tag{11}$$

where a_x is the charge transfer coefficient for anode or cathode, $i_{0,x}$ is the exchange current density for anode or cathode, i is the current density of the cell, n is the number of electrons transferred ($n = 2$).

The model uses the simplified version of Butler-Volmer equation (Eq. (12)), additionally the model neglects the cathode overvoltage because the hydrogen evolution reaction at the cathode is significantly faster than the oxygen evolution reaction at the anode [9]:

$$U_{\mathrm{act}} = \frac{\mathrm{R}T}{\mathrm{F}} \cdot \sin h^{-1}\left(\frac{i}{2i_{0,an}}\right). \tag{12}$$

The exchange current density is established using the following equation:

$$i_{0,an} = k_{i0,an} \cdot \exp\left(\frac{-E_{\mathrm{act},an}}{\mathrm{R}T}\right), \tag{13}$$

where anode activation energy $E_{\mathrm{act},an} = 76.000$ J/mol and the pre-exponential factor $k_{i0,an} = 2.16 \cdot 10^6$ A/cm^2 [9].

2.6 Ohmic overvoltage

The ohmic overvoltage is the additional voltage required to overcome the cell resistance. The resistance depends on the membrane material, thickness, hydration level, and temperature. The ohmic overvoltage can be established by the Eq. (14):

$$U_{\text{ohm}} = \left(R_{el,\text{anode}} + R_{el,\text{cathode}} + R_{mem}\right) \cdot i \cdot A_{\text{cell}}, \tag{14}$$

$$R_{el,X} = \frac{t_{el,X}}{A_{\text{cell}}} \rho_{el,X}, \tag{15}$$

$$R_{mem} = \frac{t_{mem}}{\sigma_{mem} \cdot A_{\text{cell}}}, \tag{16}$$

where $t_{el,X}$ is the electrode thickness (1 mm), $\rho_{el,X}$ is the electrode resistivity (7.5 mΩ cm) [9]. The membrane conductivity can be established by the Eq. (17):

$$\sigma_{mem} = \left(0.005139 \cdot \lambda - 0.00326\right) \cdot \exp\left(1268 \cdot \left(\frac{1}{303} - \frac{1}{T_{\text{cell}}}\right)\right), \tag{17}$$

where λ is the hydration level and is assumed to be equal to 22 [8, 9].

2.7 Concentration overvoltage

The concentration or diffusion overvoltage arises due to mass limitations in the electrolyte or at the electrode surface. The concentration overvoltage can be defined by the Eq. (18), considering only the anode side where the primary contribution is present [9]:

$$U_{conc} = \frac{\text{R} \cdot T}{\alpha_{an} \cdot n \cdot \text{F}} \cdot \ln\left(\frac{i_L}{i_L - 1}\right), \tag{18}$$

where the limiting current density i_L is considered to be equal to 6 A/cm^2 and charge transfer coefficient α_{an} is 0.5 [8, 9].

2.8 Waste heat

Heat is generated in the electrolyzer stack due to the irreversible nature of the chemical reactions and the cell's ohmic resistance [21]. While the electrolysis reaction can theoretically occur without heat exchange at the thermoneutral voltage, this results in a reaction rate that is too low to produce significant amount of hydrogen. To overcome this issue, an overvoltage is applied to the electrolyzer cells, enhancing the reaction rate and causing the reaction to release heat. The waste heat can be calculated using the Eq. (19):

$$Q_w = I \cdot \left(U_{\text{cell}} - U_{tn}\right), \tag{19}$$

where I is the current, U_{cell} is the cell voltage and U_{tn} is the thermoneutral voltage.

2.9 Mass balance

The mass transport can be calculated by the following equations:

$$\dot{m}_{\text{H}_2\text{O}} = \frac{I \cdot N_{\text{cells}}}{2 \cdot \text{F}} \cdot \eta_F \cdot M_{\text{H}_2\text{O}}, \tag{20}$$

$$\dot{m}_{\text{H}_2} = \frac{I \cdot N_{\text{cells}}}{2 \cdot \text{F}} \cdot \eta_F \cdot M_{\text{H}_2}, \tag{21}$$

$$\dot{m}_{\text{O}_2} = \frac{I \cdot N_{\text{cells}}}{4 \cdot \text{F}} \cdot \eta_F \cdot M_{\text{O}_2}, \tag{22}$$

with η_F being the Faradays efficiency, I the current, N_{cells} the number of cells in the PEM stack, $\dot{m}_x$ the mass flows and M_x the molar mass for the respective substance [7].

Assuming that the produced hydrogen is saturated with water vapor, the amount of water in the hydrogen stream can be calculated using the Eq. (23):

$$\dot{n}_{\text{H}_2\text{O } cat} = \frac{P_{sat}}{\left(P_{cat} - P_{sat}\right)} \cdot \dot{n}_{\text{H}_2}, \tag{23}$$

where P_{sat} is the water saturation pressure and P_{cat} is the cathode pressure.

2.10 Limitations

The DWSIM software [15] features an integrated "Water Electrolyzer" model. However, the "Water Electrolyzer" model in DWSIM does not support dynamic simulation. To address this limitation, a custom "PEM Electrolyzer" unit of operations has been developed. The customized "PEM Electrolyzer" operates in steady-state and does not account for thermal inertia, but is capable of running in DWSIM dynamic simulation. In the context of material balance calculations this approach is feasible because a PEM electrolyzer stack responds relatively quickly to changes in current, with a typical response time of approximately 50 ms [7]. Another limitation is that the developed model does not account for stack degradation.

The model uses cooling with the excess amount of water, the water feed is constant and adjusted to keep temperature in range 80–90 °C. The model does not account for feed water purification and preheating. The energy consumption optimization calculations take into account only the energy consumption of the stack itself.

3 Results and discussion

3.1 PEM electrolyzer technological scheme

Considering the limitations of the developed "PEM Electrolyzer" model, steady-state simulation is sufficient for simulating part-load states and energy consumption

optimization for this study. However, the ability to run the flowsheet in the dynamic mode enables real-time simulation of a varying power supply using DWSIM events feature, as well as the implementation and testing of temperature, pressure, and water level control mechanisms, while also accounting for the dynamic behavior of the oxygen and hydrogen separators.

Table 1 provides the parameters of the developed PEM electrolyzer stack model. The parameters of the balance of plant components are presented in Table 2.

The flowsheet of PEM electrolysis process developed in DWSIM is shown in Fig. 1.

Preheated water from the tank "TANK-1" is delivered to the pump "PUMP-1" and then cooled by a cooler "CL-1" to 80 °C before being supplied to the PEM electrolyzer "PEME-1" at a pressure of 2 bars. The input power of the "PEME-1" is controlled with the input energy stream "E-2".

The current and voltage of the "PEME-1" are calculated based on the input power, as detailed in Section 3.2. The "PEME-1" outlet material stream "H_2 – 1" is a hydrogen rich stream at a pressure of 30 bar, while the "$H_2O + O_2$ – 1" outlet material stream is a mixture of oxygen gas and excess amount of water at a pressure of 2 bar. The waste heat is removed by the excess water which is supplied in sufficient amount to ensure that the outlet stream "$H_2O + O_2$ – 1" temperature remains within the range of 80 to 90 °C. The hydrogen separator "SEP H_2" is used to separate hydrogen from water vapor. The purity of the obtained product (stream "H_2-PROD") is 99.9%. The liquid water stream SEP H_2_REC-1 is recycled. The oxygen separator "V-2" is used to separate oxygen from liquid water. The liquid water stream SEP O_2_REC-1 is recycled. PID controllers are used to control operating temperature, pressure and separators' water level. The parameters of PID controllers are shown in Table 3.

Energy flow of the input energy stream "E-2" is controlled with a dynamics manager event set. The power consumption schedule is calculated as detailed in Section 3.4.

Table 1 PEM electrolyzer stack parameters

Parameter		Value	Unit
Maximum power input	P_{el}	1	MW
Number of cells	n	182	-
Cell area	A	1000	cm^2
Maximum operating current density	i_{max}	2.5	A/cm^2
Maximum operating cell voltage	$V_{cell,max}$	2.2	V
Cathode pressure	P_{cat}	30	bar
Anode pressure	P_{an}	2	bar
Operating temperatures	T	60–80	°C
Water feed	m_{H_2O}	32040	kg/h

Table 2 Balance of plant components

Component	Name	Parameter	Value	Unit
Hydrogen gas-liquid separator	SEP H_2	Operating temperature	25	°C
		Operating pressure	30	bar
		Volume	0.5	m^3
		Height	1.5	m
Oxygen gas-liquid separator	SEP O_2	Operating temperature	80–90	°C
		Operating pressure	2	bar
		Volume	10	m^3
		Height	4	m
Water tank	TANK-1	Volume	10	m^3
		Height	4	m
Pump	PUMP-1	Outlet pressure	2	bar
		Efficiency	75	%

3.2 Polarization curve

The polarization curve depicts the relationship between cell voltage and current density. The parameters used for the calculation of the polarization curve are provided in Table 4.

The polarization curve of the PEM electrolyzer cell at different operating temperatures is shown in Fig. 2. The effect of operating temperature becomes significant at higher current densities. With the rise of the temperature the required cell voltage decreases.

For the custom DWSIM "PEM Electrolyzer" model, the voltage and current are calculated from the input energy stream. The calculation of the current-to-power relationship is based on the non-linear least squares method and is derived from the Eq. (24):

$$I = a \cdot P^2 + b \cdot T^2 + c \cdot P \cdot T + d \cdot P + e \cdot T + f, \quad (24)$$

with I being the current [A], P the power input [kW], T the operating temperature [°C] and a, b, c, d, e, f the set of fit parameters. The calculated fit parameters are presented in Table 5.

Fig. 3 shows the graphs of the dependence of the actual current density and the fit current density (calculated according to the Eq. 24) on input power. As shown in Fig. 4 the maximum normalized current density error does not exceed 0.8%.

3.3 PEM electrolyzer performance

The dependence of hydrogen production rate on input power was calculated for temperatures ranging from 60 to 80 °C using sensitivity analysis tool in DWSIM (Fig. 5).

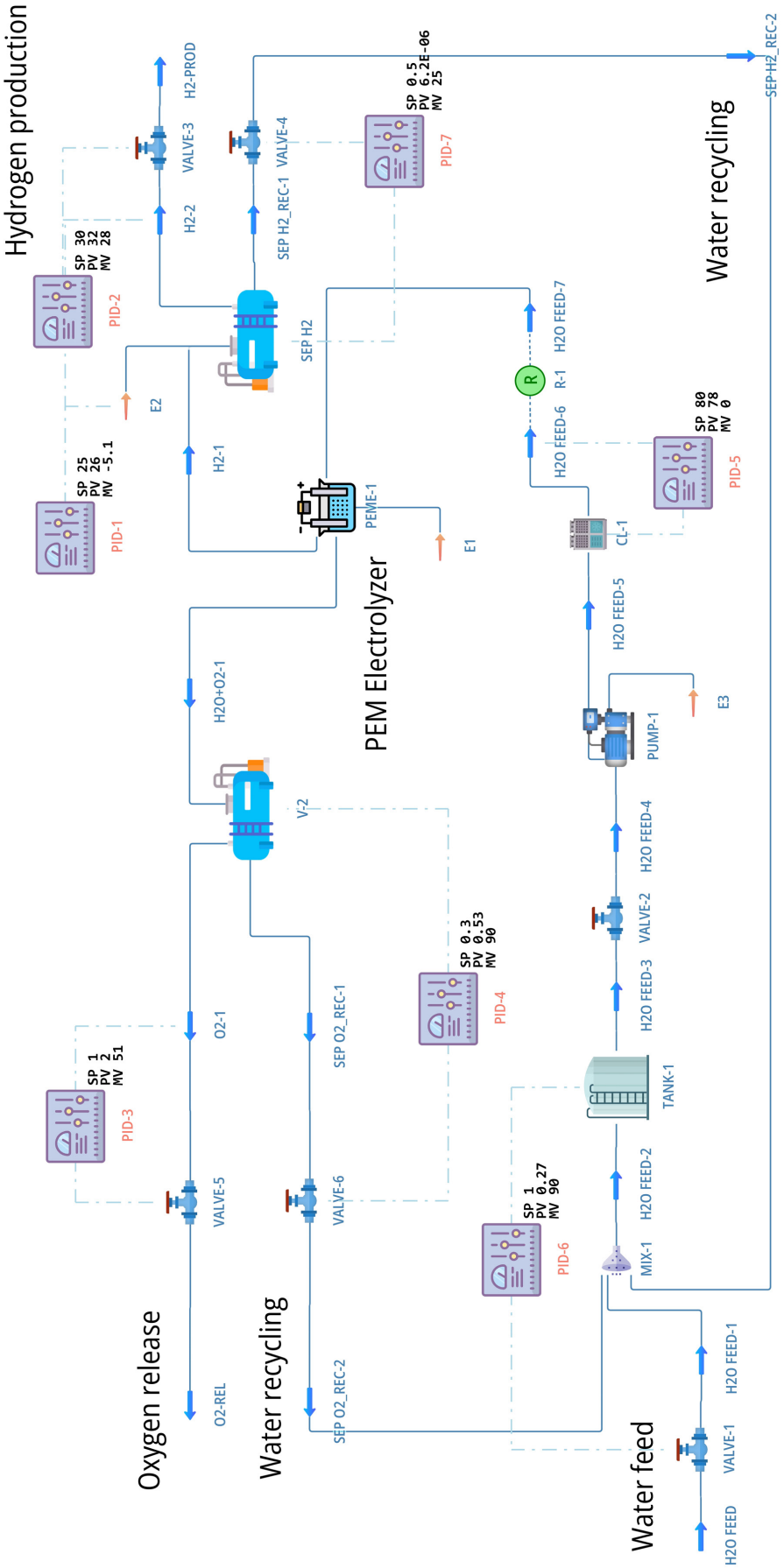

Fig. 1 PEM electrolysis DWSIM flowsheet

Table 3 PID controllers

Name	Controlled property	Manipulated property	Target value	Unit
PID-1	H_2–2 Temperature	E2 Energy flow	25	°C
PID-2	H_2–2 Pressure	VALVE-3 Opening	30	bar
PID-3	O_2–1 Pressure	VALVE-5 Opening	1	bar
PID-4	V-2 Liquid level	VALVE-6 Opening	1.5	m
PID-5	H_2O FEED-6 Temperature	CL-1 Heat removed	80	°C
PID-6	TANK-1 Liquid level	VALVE-1 Opening	1.5	m
PID-7	SEP H_2 Liquid level	VALVE-4 Opening	0.5	m

Table 4 Polarization curves parameters

Parameter		Value	Unit	Ref
Activity of water in liquid state	a_{H_2O}	1	-	[7]
Anode activation energy	$E_{act,an}$	76000	J/mol	[9]
Pre-exponential factor	$k_{i0,an}$	$2.16 \cdot 10^6$	A/cm²	[9]
Electrode thickness	t_{el}	1	mm	[9]
Electrode resistivity	$V_{cell,max}$	7.5	mΩ cm	[8, 9]
Hydration level	λ	22	-	[8, 9]
Anode charge transfer coefficient	a_n	0.5	-	[9]
Limiting current density	i_L	6	A/cm²	[9]
Faradays efficiency	η_F	1	-	[7]

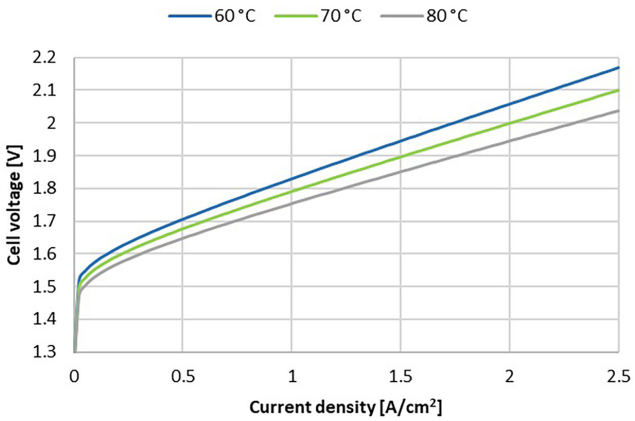

Fig. 2 Polarization curves at various operating temperature

The performance of the PEM electrolyzer is evaluated with the specific energy consumption versus input power (Fig. 6). The specific energy consumption is calculated using the Eq. (25):

$$\mathrm{SEC} = \frac{E}{m_{H2}}, \tag{25}$$

Table 5 Fit parameters

Fit parameter	Value
a	–6.525e–04
b	–5.252e–03
c	6.535e–03
d	2.7472
e	0.603
f	3.952

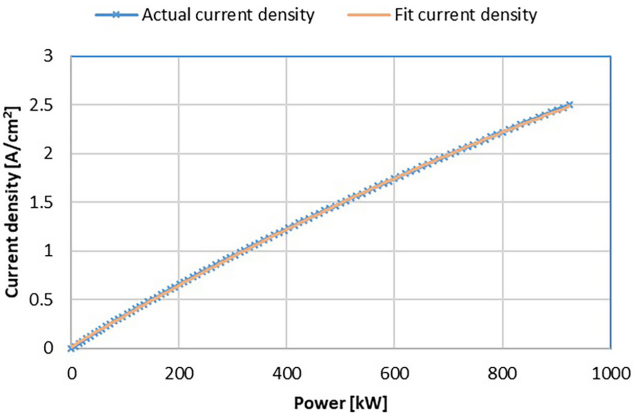

Fig. 3 Actual current density vs fit current density

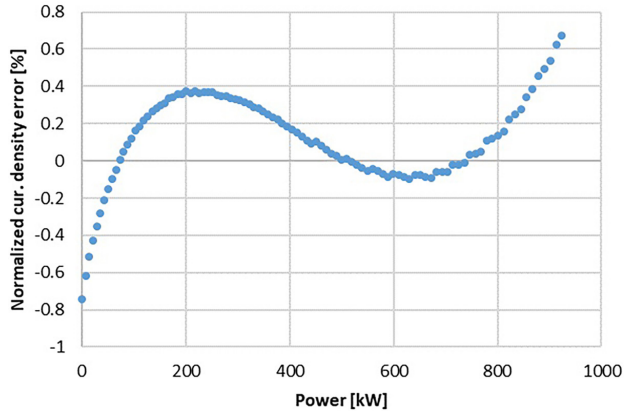

Fig. 4 Normalized current density error

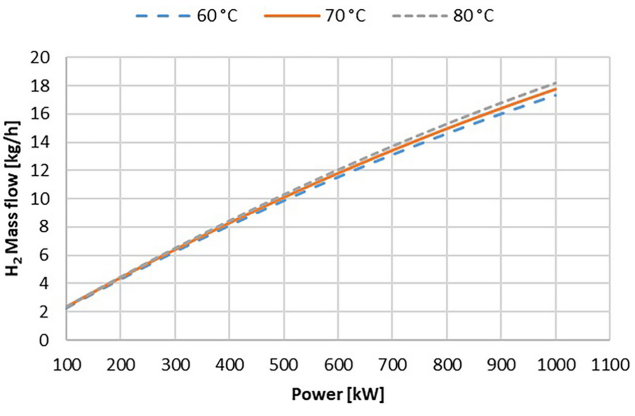

Fig. 5 H_2 production rate at various operating temperatures

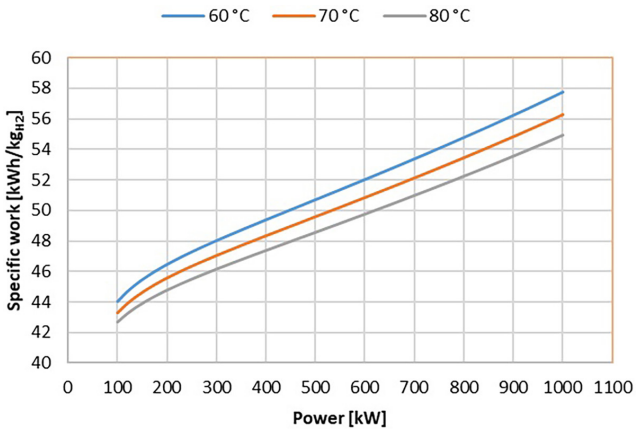

Fig. 6 Specific work vs power

where E is consumed by the PEM stack amount of energy [kWh] and m_{H2} is the amount of produced hydrogen [kg].

The specific energy consumption increases with rising input power, which in turn increases the cell voltage and subsequently the overpotentials. With rising the operating temperature, the specific energy consumption decreases.

3.4 Optimization of electricity consumption based on variable electricity prices

This section focuses on a practical example of optimizing electricity consumption to minimize costs for hydrogen production, given variable electricity prices throughout the day. The objective is to minimize the total cost of electricity while meeting the hydrogen production target of 360 kg/day. The operating conditions of the modeled PEM electrolyzer are presented in Table 6.

Daily maximum electricity rates according to the National Energy and Utilities Regulatory Commission of Ukraine [22], energy consumption and total prices for three energy consumptions strategies are presented in Table 7.

To determine the most cost-effective electricity consumption schedule, the Sequential Least Squares Quadratic Programming method was used. Table 7 provides a comparison for three energy consumption modes. The "Fixed" mode uses a constant energy consumption value. In the "Min/max" mode, the highest energy consumption takes place during the hours with the lowest tariff, this method is based on greedy algorithm with further optimization using brute force method and represents a straightforward approach for possible energy consumption optimization. These two methods are used to illustrate the difference in specific energy consumption and production price when compared to the "SLSQP" optimization method. In the "SLSQP" mode, energy consumption is calculated using Sequential Least Squares Quadratic Programming. The "SLSQP" mode is the most cost-effective, however calculations for the provided maximum electricity rates shows that "Fixed" method has the lowest specific energy consumption in this case.

The Table 8 presents data on energy consumption and price to produce 360 kg of hydrogen for the SLSQP mode at temperatures ranging from 60 to 80 °C, based on the actual tariff for 13.10.2024 with hourly prices in Ukraine for time range 00:00 – 23:00: [257, 2550, 100, 100, 100, 100, 98, 1323, 3150, 3150, 2736, 2650, 2160, 1700, 1650, 1650, 2000, 5975, 8949.49, 9000, 9000, 9000, 8950.64, 5180] (UAH/kWh). The Table 9 presents data on energy consumption and price for the SLSQP mode

Table 6 PEM electrolyzer operating conditions

Parameter		Value	Unit
Power input	P_{el}	185 – 925	kW
Operating current density	i	0.6 – 2.5	A/cm^2
Operating cell voltage	$V_{cell,max}$	1.7 – 2	V
Cathode pressure	P_{cat}	30	bar
Anode pressure	P_{an}	2	bar
Operating temperature	T	80	°C

Table 7 Daily electricity rates, energy consumption, total price

Hours	Electricity rates [UAH/kWh]	Energy consumption [kWh]		
		Fixed	Min/max	SLSQP
00:00–07:00	5.6	779.75	925	925
07:00–11:00	6.9	779.75	925	903.96
11:00–17:00	5.6	779.75	925	925
17:00–23:00	9	779.75	404.115	416.5
23:00–00:00	6.9	779.75	925	903.96
Total energy consumption [kWh]:		**18714**	**19074.69**	**19043.8**
Specific energy consumption [kWh/kg]:		**51.98**	**52.99**	**52.9**
Production price [UAH]:		**125773.67**	**121074.71**	**121017.62**

Table 8 Energy consumption and total price for temperatures 60–80 °C

Temperatures [°C]	Total energy consumption [kWh]	Specific energy consumption [kWh/kg]	Price per kg [UAH/kg]
60	20078.56	55.77	156.56
65	19823.95	55.07	150.21
70	19584.21	54.40	144.23
75	19357.79	53.77	138.59
80	19143.44	53.18	133.24

Table 9 Energy consumption and total price for production range 180–360 kg of H_2 at temperature 80 °C

H_2 produced [kg]	Total energy consumption [kWh]	Specific energy consumption [kWh/kg]	Price per kg [UAH/kg]
200	10049.34	50.25	86.87
240	12336.07	51.40	89.10
280	14580.84	52.07	95.55
320	16958.32	52.99	105.44
360	19143.44	53.18	133.24

at temperature 80 °C for hydrogen production range 200–360 kg for the same tariff.

The obtained results show that with the rise of temperature from 60 to 80 °C the specific energy consumption and the hydrogen production cost decreases. Lowering the hydrogen production demand significantly lowers the specific energy consumption and the hydrogen production price. At low hydrogen demand, the electrolyzer can operate more flexibly at part-load conditions, enabling more efficient utilization of periods with low electricity prices. With the rise of hydrogen production demand the specific energy consumption increases as the electrolyzer has to operate at higher current densities, and the effect of overpotentials increases.

4 Conclusion

A comprehensive model of a PEM electrolyzer has been developed to simulate performance at various load conditions. One of the key outcomes of this study is the identification of the most cost-effective energy consumption mode, demonstrating the model's practical application in optimizing the operation of PEM electrolyzers. This finding provides valuable insights for improving the efficiency and economic viability of hydrogen production processes under varying load conditions. Future work should build on these results by exploring further optimization strategies and validating the model against experimental data to enhance its predictive accuracy and utility in real-world applications.

Acknowledgement

The project presented in this article is supported by Department of Chemical Engineering and Ecology of Volodymyr Dahl East Ukrainian National University.

References

[1] Vidas, L., Castro, R. "Recent developments on hydrogen production technologies: State-of-the-art review with a focus on green-electrolysis", Applied Sciences, 11(23), 11363, 2021. https://doi.org/10.3390/app112311363

[2] Pareek, A., Dom, R., Gupta, J., Chandran, J., Adepu, V., Borse, P. H. "Insights into renewable hydrogen energy: Recent advances and prospects", Materials Science for Energy Technologies, 3, pp. 319–327, 2020. https://doi.org/10.1016/j.mset.2019.12.002

[3] Gavrailov, D. Y., Boycheva, S. V. "Study assessment of water electrolysis systems for green production of pure hydrogen and natural gas blending", IOP Conference Series: Earth and Environmental Science, 1234(1), 012004, 2023. https://doi.org/10.1088/1755-1315/1234/1/012004

[4] Anim-Mensah, A., Drouiche, N., Boulaiche, W. "Assessment of the economic viability, environmental, and social impacts of green hydrogen production: an Algerian case study", Frontiers in Membrane Science and Technology, 3, 1382651, 2024. https://doi.org/10.3389/frmst.2024.1382651

[5] Megía, P. J., Vizcaíno, A. J., Calles, J. A., Carrero, A. "Hydrogen production technologies: From fossil fuels toward renewable sources. A mini review", Energy and Fuels, 35(20), pp. 16403–16415, 2021. https://doi.org/10.1021/acs.energyfuels.1c02501

[6] Olivier, P., Bourasseau, C., Bouamama, B. "Low-temperature electrolysis system modelling: A review", Renewable and Sustainable Energy Reviews, 78, pp. 280–300, 2017. https://doi.org/10.1016/j.rser.2017.03.099

[7] Pfennig, M., Schiffer, B., Clees, T. "Thermodynamical and electrochemical model of a PEM electrolyzer plant in the megawatt range with a literature analysis of the fitting parameters", International Journal of Hydrogen Energy, 2024. https://doi.org/10.1016/j.ijhydene.2024.04.335

[8] Colbertaldo, P., Gómez Aláez, S. L., Campanari, S. "Zero-dimensional dynamic modeling of PEM electrolyzers", Energy Procedia, 142, pp. 1468–1473, 2017. https://doi.org/10.1016/j.egypro.2017.12.594

[9] Crespi, E., Guandalini, G., Mastropasqua, L., Campanari, S., Brouwer, J. "Experimental and theoretical evaluation of a 60 kW PEM electrolysis system for flexible dynamic operation", Energy Conversion and Management, 277, 116622, 2023. https://doi.org/10.1016/j.enconman.2022.116622

[10] MathWorks "Simulink, (10.5)", [computer program] Available at: https://www.mathworks.com/products/simulink.html [Accessed: 17 October 2024]

[11] Scheepers, F., Stähler, M., Stähler, A., Müller, M., Lehnert, W. "Cost-optimized design point and operating strategy of polymer electrolyte membrane electrolyzers", International Journal of Hydrogen Energy, 48(33), pp. 12185–12199, 2023. https://doi.org/10.1016/j.ijhydene.2022.11.288

[12] Aki, H., Sugimoto, I., Sugai, T., Toda, M., Kobayashi, M., Ishida, M. "Optimal operation of a photovoltaic generation-powered hydrogen production system at a hydrogen refueling station", International Journal of Hydrogen Energy, 43(32), pp. 14892–14904, 2018. https://doi.org/10.1016/j.ijhydene.2018.06.077

[13] Zhang, H., Yuan, T. "Optimization and economic evaluation of a PEM electrolysis system considering its degradation in variable-power operations", Applied Energy, 324. 119760, 2022. https://doi.org/10.1016/j.apenergy.2022.119760

[14] Xu, Y., Chen, H. "Layered power scheduling optimization of PV hydrogen production system considering performance attenuation of PEMEL", Global Energy Interconnection, 6(6), pp. 714–725, 2023. https://doi.org/10.1016/j.gloei.2023.11.005

[15] Daniel Medeiros "DWSIM, (8.7.1)", [computer program] Available at: https://dwsim.org/ [Accessed: 17 October 2024]

[16] Renner, J., Ayers, K., Anderson, E. "Proton exchange membrane electrolyzer stack and system design", In: PEM Electrolysis for Hydrogen Production, CRC Press, 2015, pp. 169–190. ISBN 9780429183607

[17] Shiva Kumar, S., Himabindu, V. "Hydrogen production by PEM water electrolysis – A review", Materials Science for Energy Technologies, 2(3), pp. 442–454, 2019. https://doi.org/10.1016/j.mset.2019.03.002

[18] Li, W., Tian, H., Ma, L., Wang, Y., Liu, X., Gao, X. "Low-temperature water electrolysis: fundamentals, progress, and new strategies", Materials Advances, 3(14), pp. 5598–5644, 2022. https://doi.org/10.1039/d2ma00185c

[19] Hernández-Gómez, Á., Ramirez, V., Guilbert, D. "Investigation of PEM electrolyzer modeling: Electrical domain, efficiency, and specific energy consumption", International Journal of Hydrogen Energy, 45(29), pp. 14625–14639, 2020. https://doi.org/10.1016/j.ijhydene.2020.03.195

[20] Roy, A., Watson, S., Infield, D. "Comparison of electrical energy efficiency of atmospheric and high-pressure electrolysers", International Journal of Hydrogen Energy, 31(14), pp. 1964–1979, 2006. https://doi.org/10.1016/j.ijhydene.2006.01.018

[21] van der Roest, E., Bol, R., Fens, T., van Wijk, A. "Utilisation of waste heat from PEM electrolysers – Unlocking local optimisation", International Journal of Hydrogen Energy, 48(72), pp. 27872–27891, 2023. https://doi.org/10.1016/j.ijhydene.2023.03.374

[22] National Energy and Utilities Regulatory Commission of Ukraine "On the maximum prices in the day-ahead market, intra-day market, and balancing market", [online] Available at: https://www.nerc.gov.ua/acts/pro-granichni-cini-na-rinku-na-dobu-napered-vnutrishnodobovomu-rinku-ta-balansuyuchomu-rinku-2 [Accessed: 17 October 2024]